Nuclear Physics B270 [FS16] (1986) 399–422
North-Holland, Amsterdam

FIRST-ORDER PHASE TRANSITION IN THE 3D XY MODEL WITH MIXED ACTION

W. JANKE

Freie Universität Berlin, Institut für Theorie der Elementarteilchen, Arnimallee 14, 1000 Berlin 33, F.R. Germany

H. KLEINERT[1]

Department of Physics, University of California, San Diego, La Jolla, CA 92093

Received 19 July 1985
(Revised 3 January 1986)

We show that the 3D XY model with a mixed action $\sum_{x,i}(\beta\cos(\nabla_i\theta)+\gamma\cos(2\nabla_i\theta))$ which has XY and Ising phase transitions for small and large γ, respectively, possesses a short piece of first-order transition between $\gamma\approx 0.3$ and $\gamma\approx 0.4$. Thus, no radial degrees of freedom are necessary to reach a tricritical point either in the XY model or in the lattice superconductor.

1. Introduction

First-order transitions in lattice models with continuous symmetry have recently attracted increasing attention. The main theoretical reason for this lies in the desire for a better understanding of the so-called Coleman-Weinberg or Halperin, Lubensky and Ma mechanism [1]. The practical importance ranges from cosmological issues such as the inflationary universe [2] to solid state phenomena such as liquid crystal and melting transitions [3]. According to the above mechanism, fluctuations of gauge fields coupled via the covariant derivative term $|(\partial-ieA)\psi|^2$ to a complex $g|\psi|^4$ theory can drive the phase transition first order at a *positive* coupling constant g (for a negative g it is trivially first order). The arguments for this are two-fold. On the one hand, the fluctuation determinant of the gauge field in a very smooth background field $|\psi|$ produces a term $-|\psi|^3$ or $|\psi|^4\log|\psi|$ in $D=3$ or $D=4$ dimensions, respectively. This leads to a first-order transition in the effective potential. On the other hand, the perturbatively calculated renormalization group trajectories in the g, e^2 plane have no infrared stable fixed point.

[1] Supported in part by Deutsche Forschungsgemeinschaft under grant no. Kl 256.
On sabbatical leave from Freie Universität Berlin, Institut für Theorie der Elementar-Seilchen, Arnimallee 14, 1000 Berlin 33, FRG.

0550-3213/86/$03.50 © Elsevier Science Publishers B.V.
(North-Holland Physics Publishing Division)

Some time ago it was pointed out that for $e^2 \ll g$, the smoothness assumption for $|\psi|$ in the determinantal arguments breaks down because of the presence of macroscopic fluctuations in the form of vortex lines [4]. Along the cores of these lines, the $|\psi|$ field vanishes. A field whose average is non-zero but which is threaded by many lines of zeros can no longer be smooth. By formulating a *disorder* field theory for the vortex lines it was possible to show that the theory undergoes a second order transition after all [5]. In the g, e^2 plane this implies that there must exist an infrared stable fixed point if the trajectory starts out with sufficiently small slope e^2/g. The stabilization is achieved by the *nonperturbative* character of vortex lines whose influence cannot be expanded in a power series in e^2 and g. The transition starts out to be of second order for small enough e^2/g and turns first order as soon as e^2/g exceeds a certain tricritical value [4].

A first attempt [6] to find the tricritical point by Monte Carlo simulation was undertaken in three dimensions on a lattice superconductor, which is an XY model coupled to an abelian gauge field. This attempt failed. From the analytic calculations in ref. [4] (which incidentally reproduced the Monte Carlo data quite well via simple mean-field techniques) we have learned the reason for this: the renormalized ψ^4 coupling is so large that e^2/g cannot possibly reach the tricritical ratio $e^2/g \approx 0.7/\sqrt{2}$. Indeed, when smaller values of g were admitted by using scalar fields with radial degrees of freedom [7], Monte Carlo simulations did show a first-order transition.

For simulation purposes it is useful to realize that the extension by radial degrees of freedom which greatly increases computer costs, is not really necessary. The theoretical work [4] has shown that the lattice superconductor can be modified to produce a first-order transition without such an extension. We merely have to introduce local (annealed) gaussian fluctuations of the reduced temperature of the XY model. At the mean-field level this leads to a decrease in the quartic coupling constant g thereby diminishing also the renormalized value of this coupling. When applied to the disorder version of the lattice superconductor, which is a simple XY model, this procedure leads (as we shall demonstrate in the next section) to a mixed action of the type

$$\sum_{x,i} \left(\beta \cos(\nabla_i \theta) + \delta \cos^2(\nabla_i \theta) \right), \tag{1}$$

whose partition function can be written as follows

$$Z = \prod_x \int_{-\pi}^{\pi} \frac{\mathrm{d}\theta(x)}{2\pi} \exp\left[\sum_{x,i} \left(\beta \cos(\nabla_i \theta) + \gamma \cos(2 \nabla_i \theta) \right) \right]. \tag{2}$$

By mean-field techniques it was argued that for larger γ there is a sign change in the effective quartic interaction of this theory which therefore undergoes a first-order transition.

It is the purpose of this paper to confirm this argument. We shall first give a detailed mean-field analysis of the full phase diagram and exhibit the first-order regime in the β, γ plane. Then we perform Monte Carlo simulations and verify that near the point of maximal transition entropy at the mean-field level ($\gamma \approx 0.4$) the fully fluctuating theory also has a first-order transition.

For $\gamma \gg 0.4$ the transition softens with increasing γ. The same thing happens for $\gamma \leqslant 0.2$ with decreasing γ, similar to what was observed previously in U(1) lattice gauge models [9] with mixed actions and analysed theoretically in ref. [10].

Our result should be useful in the light of recent Monte Carlo studies of Higgs models in four dimensions [8]. The existence of a tricritical point in a model like (2) which does not contain radial degrees of freedom can greatly improve the available statistics.

2. Mean-field analysis

2.1. GENERAL CONSIDERATIONS

As mentioned in the introduction, the mixed action may be viewed as the result of local (annealed) temperature fluctuations in the pure XY model. Using a gaussian distribution this is easily seen by a quadratic completion

$$\begin{aligned}
Z(\beta,\gamma) &= \prod_{x,i} \int_{-\infty}^{\infty} \frac{\mathrm{d}\beta_i(x)}{\sigma\sqrt{2\pi}} \exp\left(-\sum_{x,i} \frac{1}{2}\left(\frac{\beta_i(x)-\beta}{\sigma}\right)^2\right) Z_{\mathrm{XY}}(\beta_i(x)) \\
&= \prod_{x,i} \int_{-\infty}^{\infty} \frac{\mathrm{d}\beta_i(x)}{\sigma\sqrt{2\pi}} \prod_{x} \int_{-\pi}^{\pi} \frac{\mathrm{d}\theta(x)}{2\pi} \\
&\quad \times \exp\left(\sum_{x,i} \left[\beta_i(x) \cos \nabla_i\theta(x) - \frac{1}{2}\left(\frac{\beta_i(x)-\beta}{\sigma}\right)^2\right]\right) \\
&= \prod_{x} \int_{-\pi}^{\pi} \frac{\mathrm{d}\theta(x)}{2\pi} \exp\left(\sum_{x,i} \left[\beta \cos \nabla_i\theta(x) + \tfrac{1}{2}\sigma^2 [\cos \nabla_i\theta(x)]^2 \right]\right) \\
&= \prod_{x} \int_{-\pi}^{\pi} \frac{\mathrm{d}\theta(x)}{2\pi} \exp\left(\sum_{x,i} \left[\beta \cos(\nabla_i\theta(x)) + \gamma \cos(2\nabla_i\theta(x)) + \gamma \right]\right), \quad (3)
\end{aligned}$$

where $\gamma = \frac{1}{4}\sigma^2$ is proportional to the variance of the (inverse) temperature fluctuations. Applying this averaging to the field theoretic formulation of the pure XY model, for large enough γ, we can easily convince ourselves that the quartic bare coupling becomes negative. Hence at the mean-field level, the XY transition changes from continuous to first order. It is useful to see this in more detail. Recall the derivation of the XY field theory [11]. Changing to complex variables

$$U(x) = \mathrm{e}^{i\theta(x)},$$

the partition function can be written as

$$Z_{\rm XY}(\beta)=\prod_{x}\int_{-\pi}^{\pi}\frac{\mathrm{d}\,\theta(x)}{2\pi}\exp\Big(\tfrac{1}{2}\beta\sum_{x,i}\left[U(x)U(x+i)^{*}+\text{c.c.}\right]\Big). \tag{4}$$

Introducing an unconstrained complex field u via

$$\prod_{x}\int_{-\infty}^{\infty}\mathrm{d}u\,\mathrm{d}u^{*}\prod_{x}\delta(u-U)\,\delta(u^{*}-U^{*})f(u,u^{*})=f(U,U^{*}) \tag{5}$$

and representing the δ-functions as

$$\delta(u-U)\,\delta(u^{*}-U^{*})=\int_{-i\infty}^{i\infty}\frac{\mathrm{d}\alpha\,\mathrm{d}\alpha^{*}}{(2\pi)^{2}}\exp\left(-\tfrac{1}{2}\left[\alpha(u-U)+\text{c.c.}\right]\right), \tag{6}$$

one arrives at

$$Z_{\rm XY}(\beta)=\prod_{x}\int_{-\infty}^{\infty}\mathrm{d}u\,\mathrm{d}u^{*}\prod_{x}\int_{-i\infty}^{i\infty}\frac{\mathrm{d}\alpha\,\mathrm{d}\alpha^{*}}{(2\pi)^{2}}$$
$$\times\exp\Big(\tfrac{1}{2}\sum_{x,i}\beta\left[u(x)u(x+i)^{*}+\text{c.c.}\right]-\tfrac{1}{2}\sum_{x}\left[\alpha u+\text{c.c.}\right]+\sum_{x}\ln I_{0}(|\alpha|)\Big), \tag{7}$$

where the Bessel function I_0 is the result of the one-link integral

$$\prod_{x}\int_{-\pi}^{\pi}\frac{\mathrm{d}\theta}{2\pi}\exp\Big(\tfrac{1}{2}\sum_{x}\left[\alpha U+\text{c.c.}\right]\Big)=\prod_{x}\int_{-\pi}^{\pi}\frac{\mathrm{d}\theta}{2\pi}\exp\Big(\sum_{x}|\alpha|\cos\theta\Big)$$
$$=\prod_{x}I_{0}(|\alpha|). \tag{8}$$

Local gaussian fluctuations in $\beta_i(x)$ with variance $\sigma^2=4\gamma$ then lead to

$$Z(\beta,\gamma)=\prod_{x}\int_{-\infty}^{\infty}\mathrm{d}u\,\mathrm{d}u^{*}\prod_{x}\int_{-i\infty}^{i\infty}\frac{\mathrm{d}\alpha\,\mathrm{d}\alpha^{*}}{(2\pi)^{2}}$$
$$\times\exp\Big(\sum_{x,i}\Big(\beta\left[\tfrac{1}{2}(u(x)u(x+i)^{*}+\text{c.c.})\right]+2\gamma\left[\tfrac{1}{2}(u(x)u(x+i)^{*}+\text{c.c.})\right]^{2}\Big)\Big)$$
$$\times\exp\Big(-\tfrac{1}{2}\sum_{x}(\alpha u+\text{c.c.})+\sum_{x}\ln I_{0}(|\alpha|)\Big)$$
$$\equiv\mathrm{e}^{-\beta F}. \tag{9}$$

In the mean-field approximation one looks for constant real saddle-points of the free energy (per site)

$$\beta f = \beta F/N = -D\beta u^2 - 2D\gamma u^4 + \alpha u - \ln I_0(\alpha) - D\gamma . \tag{10}$$

At these minima, u can be replaced by

$$u = \frac{I_1(\alpha)}{I_0(\alpha)} = \tfrac{1}{2}\alpha - \tfrac{1}{2}\left(\tfrac{1}{2}\alpha\right)^3 + \dots \tag{11}$$

and expanding $\ln I_0$ to the same order in α

$$\ln I_0(\alpha) = \left(\tfrac{1}{2}\alpha\right)^2 - \tfrac{1}{4}\left(\tfrac{1}{2}\alpha\right)^4 + \dots \tag{12}$$

one finds

$$\begin{aligned} \beta f &= (1 - D\beta)\left(\tfrac{1}{2}\alpha\right)^2 + \left(D\beta - \tfrac{3}{4} - 2D\gamma\right)\left(\tfrac{1}{2}\alpha\right)^4 + \dots \\ &\approx (1 - D\beta)\left(\tfrac{1}{2}\alpha\right)^2 + \left(\tfrac{1}{4} - 2D\gamma\right)\left(\tfrac{1}{2}\alpha\right)^4 + \dots . \end{aligned} \tag{13}$$

For a positive quartic term the phase transition is continuous and we can read off the mean-field transition temperature directly from the quadratic coefficient, $\beta_c^{MF} = 1/D$. For $\gamma > 1/8D$, however, the quartic coefficient becomes negative and signals the changeover to a first-order transition.

Given such a situation it is useful to perform a mean-field analysis based on an extended field formulation of the partition function in which $\cos(2\nabla_i\theta) = \frac{1}{2}[U(\boldsymbol{x})^2 U(\boldsymbol{x}+\boldsymbol{i})^{*2} + \text{c.c.}]$ is taken into account by a second set of fields v and α' [12]. Apart from the trivial fact that additional parameters always improve the accuracy of variational procedures, there are three motivations for doing so. First, additional order parameters are necessary in order that the mean-field approximation reproduces the Ising transition for large γ (which is due to the second term in the action (2) squeezing the angle θ into the two discrete values $0, \pi$). Second, only in such an extended version can the mean-field approximation be considered as the lowest order term in a systematic $(1/D)$-expansion which controls the fluctuation corrections [13]. Third, the new field has an important physical meaning. Let us recall that the field $u(\boldsymbol{x})$ in the ordinary XY model is not only an order field of this model. It also functions as *a disorder field* of oriented non-backtracking random loops which appear in the high-temperature expansion of the model. At high temperatures there are few such loops and the disorder field $u(\boldsymbol{x})$ shows this by having a vanishing expectation value. [14]. At low temperatures, the loops condense, some of them becoming infinitely long. This reflects itself in the disorder field $u(\boldsymbol{x})$ acquiring a non-zero expectation value. The advantage of having a second field $v(\boldsymbol{x})$ allows us to keep track of the strong-coupling graphs of strength-2. For $v \neq 0$, these form a condensate. This will be seen in detail later.

Introducing the fields v and α' in complete analogy to u and α in eqs. (5)–(7), we can write down directly the field representation

$$Z(\beta,\gamma)=\prod_x\int_{-\pi}^{\pi}\frac{\mathrm{d}\theta}{2\pi}\exp\Big(\sum_{x,i}\left[\beta\cos(\nabla_i\theta)+\gamma\cos(2\nabla_i\theta)\right]\Big)$$

$$=\prod_x\int_{-\infty}^{\infty}\mathrm{d}u\,\mathrm{d}u^*\,\mathrm{d}v\,\mathrm{d}v^*\prod_x\int_{-i\infty}^{i\infty}\frac{\mathrm{d}\alpha\,\mathrm{d}\alpha^*}{(2\pi)^2}\frac{\mathrm{d}\alpha'\,\mathrm{d}\alpha'^*}{(2\pi)^2}$$

$$\times\exp\Big(\tfrac{1}{2}\sum_{x,i}\left[\beta u(x)u(x+i)^*+\gamma v(x)v(x+i)^*+\text{c.c.}\right]\Big)$$

$$\times\exp\Big(-\tfrac{1}{2}\sum_x\left[\alpha u+\alpha' v+\text{c.c.}\right]+\sum_x\ln I_0(\alpha,\alpha')\Big),\tag{14}$$

where the one-link integral leads now to a somewhat generalized modified Bessel function of the two (complex) arguments α, α'

$$I_0(\alpha,\alpha')\equiv\int_{-\pi}^{\pi}\frac{\mathrm{d}\theta}{2\pi}\exp\left(\tfrac{1}{2}\left[\alpha U+\alpha' U^2+\text{c.c.}\right]\right)$$

$$=\int_{-\pi}^{\pi}\frac{\mathrm{d}\theta}{2\pi}\exp\left(|\alpha|\cos\theta+|\alpha'|\cos(2\theta+\psi)\right),\tag{15}$$

with $\psi=\arg(\alpha')-2\arg(\alpha)$. At the mean-field level we look again for constant, real saddle-points of the free energy (per site)

$$\beta f=-\frac{1}{N}\ln Z$$

$$=-\left[D\beta u^2+D\gamma v^2-\alpha u-\alpha' v+\ln I_0(\alpha,\alpha')\right].\tag{16}$$

This is extremal at

$$2D\beta u=\alpha,$$

$$2D\gamma v=\alpha',$$

$$u=\frac{\partial\ln I_0(\alpha,\alpha')}{\partial\alpha}\equiv Q_1(\alpha,\alpha'),$$

$$v=\frac{\partial\ln I_0(\alpha,\alpha')}{\partial\alpha'}\equiv Q_2(\alpha,\alpha').\tag{17}$$

Expressing u and v in terms of α and α', βf becomes

$$\beta f = \frac{\alpha^2}{4D\beta} + \frac{\alpha'^2}{4D\gamma} - \ln I_0(\alpha, \alpha'), \tag{18}$$

where $\alpha(\beta, \gamma)$, $\alpha'(\beta, \gamma)$ are the solutions of the coupled equations

$$\frac{\alpha}{D\beta} = Q_1(\alpha, \alpha'), \tag{19a}$$

$$\frac{\alpha'}{D\gamma} = Q_2(\alpha, \alpha'). \tag{19b}$$

It is worth pointing out that eq. (18) is also found by integrating out the fields $u(x)$ and $v(x)$ directly in (14). In this way we would obtain a completely equivalent field formulation of the partition function involving only the fields α, α' and (18) would be its mean-field free energy.

Notice that if in the definition of $I_0(\alpha, \alpha')$ (eq. (15)) $\theta \in [0, 2\pi]$ is replaced by $(2\pi/N)n$, $n = 0, \ldots, N-1$ and $\int_{-\pi}^{\pi} d\theta/2\pi$ by $(1/N)\Sigma_{n=0}^{N-1}$, eq. (18) gives also the mean-field energy of Z_N mixed models.

Let us now discuss the phase structure in the β, γ plane. First, we observe that

$$Q_1(\alpha, \alpha') = -Q_1(-\alpha, \alpha'), \tag{20}$$

so that as a special case

$$Q_1(0, \alpha') = 0. \tag{21}$$

Furthermore we see that

$$Q_2(\alpha, 0) = \frac{I_2(\alpha)}{I_0(\alpha)} > 0 \qquad (\alpha \neq 0). \tag{22}$$

As a consequence, eqs. (19a, b) admit three types of solutions:

$$\begin{aligned}
&\text{(i)} && \alpha = \alpha' = 0 && \text{(disordered phase (DO))}, \\
&\text{(ii)} && \alpha \neq 0, \quad \alpha' \neq 0 && \text{(ordered phase (O))}, \\
&\text{(iii)} && \alpha = 0, \quad \alpha' = D\gamma Q_2(0, \alpha') = D\gamma \frac{I_1(\alpha')}{I_0(\alpha')} \neq 0 && \text{(disordered Ising (IDO))}.
\end{aligned} \tag{23}$$

The three regimes are shown in the phase diagram in fig. 1 and the remainder of this

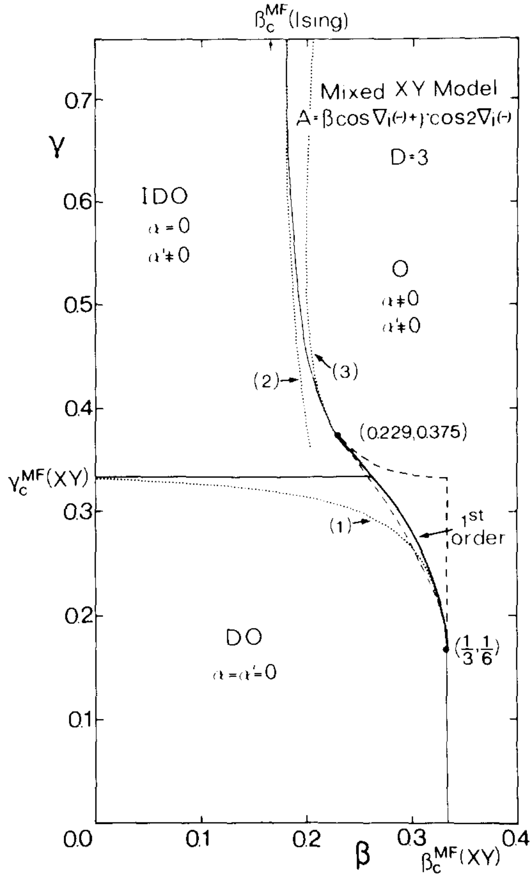

Fig. 1. The phase boundaries of the mixed action XY model $\beta\cos(\nabla_i\theta)+\gamma\cos(2\nabla_i\theta)$ in the β, γ plane as obtained from the mean-field considerations. There are three phases: ordered (O), disordered (DO) and disordered of the Ising type (IDO). The thin lines denote second order, the fat line a first order phase transition. The dashed lines are the lines of maximal undercooling and overheating, respectively. The dotted lines correspond to various approximations explained in the text: (1) small α, α' expansion, eq. (36); (2) large γ expansion of $\beta_c^{(0)}$, eq. (65); (3) $\gamma \approx \gamma_c^{MF}$ expansion of $\beta_c^{(0)}$, eqs. (62), (63).

section is devoted to the calculation of the phase boundaries. A solution with $\alpha \neq 0$, $\alpha' = 0$ is ruled out by (22).

In the dual random loop interpretation, the phases are characterized as follows: In the disordered phase (DO), the system contains practically no loops of either strength-1 or strength-2 ($u = v = 0$). During the transition to the ordered phase (DO → O), the loops of strength-1 condense which means that they become prolific with some of them acquiring infinite length ($u \neq 0$). At the same time, also the loops of strength-2 condense ($v \neq 0$). However, in counting these we have to make sure to include also those loops which split for part of their way into two branches of strength-1. Since both types of loops are oriented and non-backtracking the universality class of the transition is that of the XY model ($\hat{=}$ superfluid transition).

The disordered Ising phase (IDO) is filled from the outset with a condensate of loops of strength-2 ($v \neq 0$) and contains only a few small loops of strength-1 ($u = 0$). Thereby, the condensate of the strength-2 loops acts as a source of pairs of strength-1 loops. As a consequence it is no longer possible to assign an orientation to the latter. This is why the phase transition IDO → O is of the Ising universality class.

The transition IDO ↔ DO, finally, is once more a transition in which the oriented non-backtracking loops of strength-2 condense. This puts it into the same universality class as the transition DO → O, namely XY.

Before presenting a full numerical solution of (18), (19) it is useful to study the phase boundaries in some limiting cases.

2.2. LIMITING CASES

2.2.1. $\alpha = \alpha' = 0 \leftrightarrow \alpha = 0, \alpha' \neq 0$ *(DO ↔ IDO).* When varying γ at any β we find a continuous XY transition. Since $I_1(\alpha')/I_0(\alpha') \approx (\frac{1}{2}\alpha') + \dots$, the nontrivial solution with $\alpha' \neq 0$ sets in for $\gamma > 1/D$ (the horizontal line in fig. 1).

2.2.2. $\alpha = \alpha' = 0 \leftrightarrow \alpha \neq 0, \alpha' \neq 0$ *(DO ↔ O).* For simplicity let us limit ourselves to solutions with *small* nonzero fields α'. Then, using the expansion (for real α, α')

$$I_0(\alpha, \alpha') = I_0(\alpha) + \left(\tfrac{1}{2}\alpha'\right)2I_2(\alpha) + \left(\tfrac{1}{2}\alpha'\right)^2\left[I_0(\alpha) + I_4(\alpha)\right] + \left(\tfrac{1}{2}\alpha'\right)^3\frac{1}{3!}\left[6I_2(\alpha) + 2I_6(\alpha)\right] + \left(\tfrac{1}{2}\alpha'\right)^4\frac{1}{4!}\left[6I_0(\alpha) + 8I_4(\alpha) + 2I_8(\alpha)\right], \tag{24}$$

we see that at a minimum of βf, α' starts out as

$$\alpha' \approx \frac{I_2(\alpha)}{I_0(\alpha)} \approx \frac{\alpha^2}{4}.$$

More accurately, expanding the Bessel functions in (24)* we find, up to order α^6 (with the abbreviations $h \equiv \frac{1}{2}\alpha$, $h' \equiv \frac{1}{2}\alpha'$),

$$I_0(\alpha, \alpha') = 1 + h^2 + \tfrac{1}{4}h^4 + h'h^2 + h'^2 + \tfrac{1}{36}h^6 + \tfrac{1}{3}h'h^4 + h'^2h^2 \tag{25}$$

* $I_0(\alpha) = 1 + (\frac{1}{2}\alpha)^2 + \frac{1}{4}(\frac{1}{2}\alpha)^4 + \frac{1}{36}(\frac{1}{2}\alpha)^6 + \dots,$

$I_2(\alpha) = \frac{1}{2}(\frac{1}{2}\alpha)^2 + \frac{1}{6}(\frac{1}{2}\alpha)^4 + \dots.$

and taking the logarithm

$$\ln I_0(\alpha, \alpha') = h^2 - \tfrac{1}{4}h^4 + h'h^2 + h'^2 + \tfrac{1}{9}h^6 - \tfrac{2}{3}h'h^4 . \tag{26}$$

Notice that in (26) the contribution $\sim h'^2h^2$ happens to cancel. Differentiating $\ln I_0(\alpha, \alpha')$ with respect to α' gives the expansion of $Q_2(\alpha, \alpha')$. Thus eq. (19b) becomes

$$D\gamma h' = \tfrac{1}{2}\left[2h' + h^2 - \tfrac{2}{3}h^4 + \dots\right] \tag{27}$$

and can be solved easily for h':

$$h' = \frac{1}{2(1/D\gamma - 1)}\left[h^2 - \tfrac{2}{3}h^4 + \dots\right]. \tag{28}$$

Using this relation the expansion of the free energy

$$\beta f = \left[\frac{1}{D\beta} - 1\right]h^2 + \left[\frac{1}{D\gamma} - 1\right]h'^2 + \tfrac{1}{4}h^4 - h'h^2$$
$$- \tfrac{1}{9}h^6 + \tfrac{2}{3}h'h^4 \tag{29}$$

can be expressed as a power series in h^2 only

$$\beta f = c_2h^2 + c_4h^4 + c_6h^6 + \dots , \tag{30}$$

with coefficients

$$c_2 = \frac{1}{D\beta} - 1 ,$$
$$c_4 = \frac{1}{4}\,\frac{1 - 2D\gamma}{1 - D\gamma} ,$$
$$c_6 = \frac{1}{9}\,\frac{4D\gamma - 1}{1 - D\gamma} . \tag{31}$$

The important point is that for $1/2D \leqslant \gamma \leqslant 1/D$ the quartic coefficient c_4 becomes negative. Hence there is a tricritical point at

$$(\beta^{\mathrm{TCP}}, \gamma^{\mathrm{TCP}}) = \left(\frac{1}{D}, \frac{1}{2D}\right)$$
$$= (0.3333, 0.1667) \qquad \text{in } D = 3 . \tag{32}$$

For $\gamma \leqslant \gamma^{\mathrm{TCP}} = 1/2D$ the phase boundary is the straight line $\beta = 1/D$ (see fig. 1). For $\gamma \geqslant \gamma^{\mathrm{TCP}}$, we can follow the first-order transition to a good approximation as long as the jump in α remains small. The first-order transition takes place when the nontrivial mimimum of βf hits zero, i.e., when the solution

$$h^2 = -\frac{c_4}{2c_6} \pm \sqrt{\left(\frac{c_4}{2c_6}\right)^2 - \frac{c_2}{c_6}} \tag{33}$$

degenerates. This happens at

$$c_2 = \frac{c_4^2}{4c_6}, \tag{34}$$

with a jump in $h^2 = (\frac{1}{2}\alpha)^2$

$$h_c^2 = \frac{(-c_4)}{2c_6} = \left(\tfrac{1}{2}\alpha_c\right)^2. \tag{35}$$

Inserting the coefficients (31) we find explicit expressions for the *phase boundary*

$$\frac{1}{D\beta - 1} = \frac{9}{64} \frac{[1 - 2D\gamma]^2}{[1 - D\gamma][4D\gamma - 1]} \tag{36}$$

and the jumps of the *order parameters* across this line

$$\alpha_c^2 = \frac{9}{2} \frac{2D\gamma - 1}{4D\gamma - 1} + \dots,$$

$$\alpha_c' = \frac{9}{8} \frac{D\gamma(2D\gamma - 1)}{(1 - D\gamma)(4D\gamma - 1)} + \dots. \tag{37}$$

It is now straightforward to calculate the internal energy

$$u = \frac{\mathrm{d}}{\mathrm{d}\beta}(\beta f) = -\frac{1}{4D\beta^2}\alpha^2, \tag{38}$$

the latent heat

$$\Delta u = u(0) - u(\alpha_c) = \frac{1}{4D\beta_c^2}\alpha_c^2 \tag{39}$$

and the entropy jump

$$\Delta s = \beta_c \Delta u = \frac{1}{4D\beta_c}\alpha_c^2. \tag{40}$$

The approximate phase boundary (36) is displayed in fig. 1 as the dotted line (1). The jumps of the order parameters and entropy as functions of γ are shown in fig. 3.

2.2.3. $\alpha = 0, \alpha' \neq 0 \leftrightarrow \alpha \neq 0, \alpha' \neq 0$ (IDO $\leftrightarrow$ O). This case is slightly more involved since α' is nonzero all the way. For $\alpha = 0$, α' can be calculated from

$$\frac{\alpha'}{2D\gamma} = \frac{I_1(\alpha')}{I_0(\alpha')} \equiv q_1(\alpha') . \tag{41}$$

Let us denote the (unique) nontrivial solution of (41) by $\alpha'_0 = \alpha'_0(\gamma)$. The strategy is then to expand the free energy around $\alpha = 0$, $\alpha' = \alpha'_0$. To this end we need the expansion of $I_0(\alpha, \alpha')$ for *arbitrary* α':

$$\begin{aligned} I_0(\alpha, \alpha') &= I_0(\alpha') + \tfrac{1}{4}\alpha^2\left[I_0(\alpha') + I_1(\alpha')\right] \\ &\quad + \frac{\alpha^4}{4!}\left[\tfrac{3}{8}I_0(\alpha') + \tfrac{1}{2}I_1(\alpha') + \tfrac{1}{8}I_2(\alpha')\right] \\ &\quad + \frac{\alpha^6}{6!}\left[\tfrac{5}{16}I_0(\alpha') + \dots\right] + \dots . \end{aligned} \tag{42}$$

Taking the logarithm we find

$$\ln I_0(\alpha, \alpha') = d_0(\alpha') + d_2(\alpha')\alpha^2 + d_4(\alpha')\alpha^4 + d_6(\alpha')\alpha^6 + \dots , \tag{43}$$

where

$$\begin{aligned} d_0(\alpha') &= \ln I_0(\alpha') , \\ d_2(\alpha') &= \tfrac{1}{4}\left[1 + q_1(\alpha')\right] , \\ d_4(\alpha') &= -\tfrac{1}{64} - \tfrac{1}{24}q_1(\alpha') + \tfrac{1}{32}\left[\tfrac{1}{6}q_2(\alpha') - q_1(\alpha')^2\right] \end{aligned} \tag{44}$$

and $q_n(\alpha')$ is short for $I_n(\alpha')/I_0(\alpha')$. Writing

$$\alpha' = \alpha'_0 + \tilde{\alpha}' \tag{45}$$

and expanding the coefficients $d_n(\alpha')$ in $\tilde{\alpha}'$

$$d_n(\alpha') = \sum_{k=0} d_n^{(k)}(\alpha'_0)\frac{\tilde{\alpha}'^k}{k!} , \tag{46}$$

it is easy to see that at a minimum of βf with small α we have again

$$\tilde{\alpha}' \sim \alpha^2 . \tag{47}$$

Therefore, up to order α^6 the free energy has an expansion

$$\beta f - \beta f^{(0)} = \frac{\alpha^2}{4D\beta} + \frac{\tilde{\alpha}'^2}{4D\gamma} - \tfrac{1}{2}d_0''\tilde{\alpha}'^2 - \tfrac{1}{6}d_0'''\tilde{\alpha}'^3$$
$$-\alpha^2\left[d_2 + d_2'\tilde{\alpha}' + \tfrac{1}{2}d_2''\tilde{\alpha}'^2\right]$$
$$-\alpha^4\left[d_4 + d_4'\tilde{\alpha}'\right] - d_6\alpha^6 - \dots, \tag{48}$$

where $d_n' \equiv d_n^{(1)}(\alpha_0')$ etc., and

$$\beta f^{(0)} = \frac{\alpha_0'^2}{4D\gamma} - \ln I_0(\alpha_0') \tag{49}$$

is the free energy in the disordered phase. Minimizing with respect to $\tilde{\alpha}'$ leads to an equation for $\tilde{\alpha}'$

$$\tilde{\alpha}'\left[\frac{1}{2D\gamma} - d_0'' - d_2''\alpha^2\right] = \tfrac{1}{2}d_0'''\tilde{\alpha}'^2 + d_2'\alpha^2 + d_4'\alpha^4, \tag{50}$$

which may be solved by the ansatz

$$\tilde{\alpha}' = e\alpha^2 + d\alpha^4. \tag{51}$$

Comparing equal powers we find

$$e = \frac{d_2'}{1/2D\gamma - d_0''},$$
$$d = \frac{ed_2'' + \tfrac{1}{2}d_0'''e^2 + d_4'}{1/2D\gamma - d_0''}. \tag{52}$$

Notice that $e = e(\gamma)$, $d = d(\gamma)$ are functions of γ alone. Using (51) it is straightforward to reexpress the free energy (48) as a power series in α^2

$$\beta f - \beta f^{(0)} = c_2(\beta, \gamma)\alpha^2 + c_4(\gamma)\alpha^4 + c_6(\gamma)\alpha^6 + \dots, \tag{53}$$

with

$$c_2(\beta, \gamma) = \frac{1}{4D\beta} - d_2(\alpha_0')$$
$$= \frac{1}{4}\left[\frac{1}{D\beta} - \left(1 + \frac{I_1(\alpha_0')}{I_0(\alpha_0')}\right)\right]$$
$$= \frac{1}{4}\left[\frac{1}{D\beta} - \left(1 + \frac{\alpha_0'}{2D\gamma}\right)\right] \tag{54}$$

and

$$c_4(\gamma) = \frac{e^2}{4D\gamma} - \tfrac{1}{2}d_0''e^2 - d_2'e - d_4$$

$$= -\frac{1}{2}\frac{d_2'^2}{1/2D\gamma - d_0''} - d_4$$

$$= -\frac{1}{2}\frac{\frac{1}{16}q_1'^2}{1/2D\gamma - q_1'} + \tfrac{1}{64} + \tfrac{1}{24}q_1$$

$$- \tfrac{1}{32}\left[\tfrac{1}{6}q_2 - q_1^2\right]. \tag{55}$$

Applying recurrence formulae for Bessel functions,

$$q_1' = \left(\frac{I_1}{I_0}\right)' = 1 - \frac{q_1}{\alpha_0'} - q_1^2, \tag{56}$$

this can be simplified to

$$c_4(\gamma) = -\frac{1}{32}\frac{\left[1 - q_1/\alpha_0' - q_1^2\right]^2}{2q_1/\alpha_0' + q_1^2 - 1}$$

$$+ \tfrac{1}{64} + \tfrac{1}{24}q_1 - \tfrac{1}{32}\left[\tfrac{1}{6}q_2 - q_1^2\right]. \tag{57}$$

Moreover, using

$$q_2 = 1 - \frac{2q_1}{\alpha_0'}, \tag{58}$$

$c_4(\gamma)$ can be rewritten as a function of α_0' and $q_1(\alpha_0')$

$$c_4(\gamma) = -\frac{1}{32}\frac{\left[1 - q_1/\alpha_0' - q_1^2\right]^2}{2q_1/\alpha_0' + q_1^2 - 1} + \frac{1}{32\cdot 3} + \frac{q_1}{24} + \frac{1}{32}\left[\frac{1}{3}\frac{q_1}{\alpha_0'} + q_1^2\right]. \tag{59}$$

The tricritical value γ^{TCP} is determined by the equation $c_4(\gamma^{\mathrm{TCP}}) = 0$. In order to find this value, we first calculate α_{0c}' from (59) and then γ^{TCP} from $\gamma^{\mathrm{TCP}} = (1/2D)\alpha_{0c}'/q_1$. Using the *small* α expansion

$$q_1(\alpha) = \left(\frac{\alpha}{2}\right) - \frac{1}{2}\left(\frac{\alpha}{2}\right)^3 + \frac{1}{3}\left(\frac{\alpha}{2}\right)^5 - \frac{11}{3\cdot 2^4}\left(\frac{\alpha}{2}\right)^7$$

$$+ \frac{19}{5\cdot 3\cdot 2^3}\left(\frac{\alpha}{2}\right)^9 - \frac{473}{5\cdot 3^3\cdot 2^5}\left(\frac{\alpha}{2}\right)^{11} + \frac{6049}{7^2\cdot 5\cdot 3\cdot 2^7}\left(\frac{\alpha}{2}\right)^{13} + \dots, \tag{60}$$

which up to $\alpha \approx 1$ has a relative error less than 10^{-7}, α'_{0c} can be found on a pocket calculator quite easily by trial and error. A little more accurate computer search for the zero of $c_4(\gamma)$ gives the following tricritical values

$$\alpha'_{0c} = 1.0203\,, \tag{61a}$$

$$\gamma^{\text{TCP}} = 0.3749\frac{3}{D} \tag{61b}$$

and from $c_2(\beta^{\text{TCP}}, \gamma^{\text{TCP}}) = 0$ (see eq. (54))

$$\beta^{\text{TCP}} = 0.2293\frac{3}{D}\,. \tag{61c}$$

We now turn to the discussion of $c_2(\beta, \gamma)$. The zero of this coefficient determines a continuous transition, or in the case of a first-order transition, the undercooling temperature. Recalling (54), $c_2(\beta, \gamma) = 0$ implies

$$\beta_c^{(0)} = \frac{1}{D}\frac{1}{1 + \alpha'_0/2D\gamma}\,. \tag{62}$$

For $\gamma \lesssim 1/D$ this may be evaluated using the expansion

$$\alpha_0'^2 = 8\left(1 - \frac{1}{D\gamma}\right) + \frac{32}{3}\left(1 - \frac{1}{D\gamma}\right)^2 + \dots\,. \tag{63}$$

In the Ising limit $\gamma \to \infty$, we use the expansion

$$\alpha'_0 = 2D\gamma - \frac{1}{2} - \frac{3}{16D\gamma} - \frac{9}{64D^2\gamma^2} - \dots \tag{64}$$

to find

$$\beta_c^{(0)} = \frac{1}{2D}\left[1 + \frac{1}{8D\gamma} + \frac{1}{16(D\gamma)^2} + \frac{25}{8\cdot 64(D\gamma)^3} + \dots\right]. \tag{65}$$

This shows that for $\gamma \to \infty$ the mean-field approximation of the mixed XY model reproduces the Ising transition at $\beta_c^{(0)} = 1/(2D)$. From the dotted line (2) in fig. 1 we see that this large γ approximation is very accurate down to $\gamma \approx 0.5$. $\beta_c^{(0)}$ evaluated with the $\gamma \approx \gamma_c^{\text{MF}}$ approximation (63) is shown as dotted line (3).

2.3. NUMERICAL SOLUTION

In this section we describe the numerical minimization of

$$\beta f = \frac{\alpha^2}{4D\beta} + \frac{\alpha'^2}{4D\gamma} - \ln I_0(\alpha, \alpha')\,. \tag{66}$$

For fixed β and γ this is quite tedious since near a first-order transition, βf has two minima of roughly the same depth. A few level plots of $\beta f(\alpha, \alpha')$ were useful in order to get some feeling for the α, α' landscape. For the accurate determination of the phase boundaries we used the following algorithm: At fixed γ we choose a fixed $\alpha \neq 0$ and calculate α' from

$$\frac{\alpha'}{2D\gamma} = \frac{I_2(\alpha, \alpha')}{I_0(\alpha, \alpha')} \tag{67}$$

by iteration. Since $I_2(\alpha, \alpha')/I_0(\alpha, \alpha')$ is strictly positive for $\alpha \neq 0$ and monotonic increasing, this equation has always a nontrivial, unique solution. Then, with α, α' known, β follows from

$$\beta = \frac{\alpha}{2D} \bigg/ \frac{I_1(\alpha, \alpha')}{I_0(\alpha, \alpha')} . \tag{68}$$

Inserting $\gamma, \alpha, \alpha', \beta$ in (66) we finally determine the free energy. In practice, we start from large α, go through the steps described above to find $\alpha', \beta, \beta f$ and keep repeating all steps for decreasing values of α. The resulting curve for βf is shown for $\gamma = 0.25$ in fig. 2. The procedure has to be repeated for various values of γ. The full

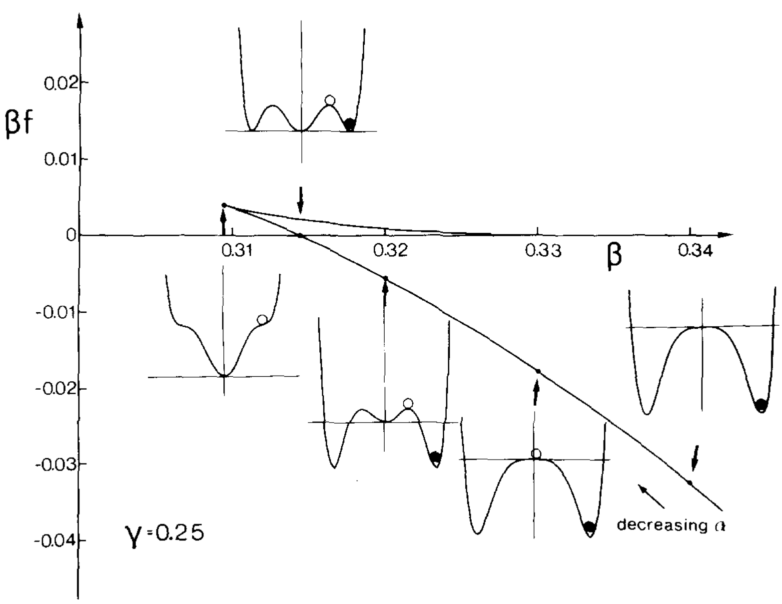

Fig. 2. Illustration of mean-field evaluation of the first-order transition point at $\gamma = 0.25$. The plot shows βf as a function of β traced out by varying the extremal value of α from large to zero value. This results in two branches, one where α sits at a maximum and one where it sits at a minimum. The extremal point on the left is the point of maximal overheating.

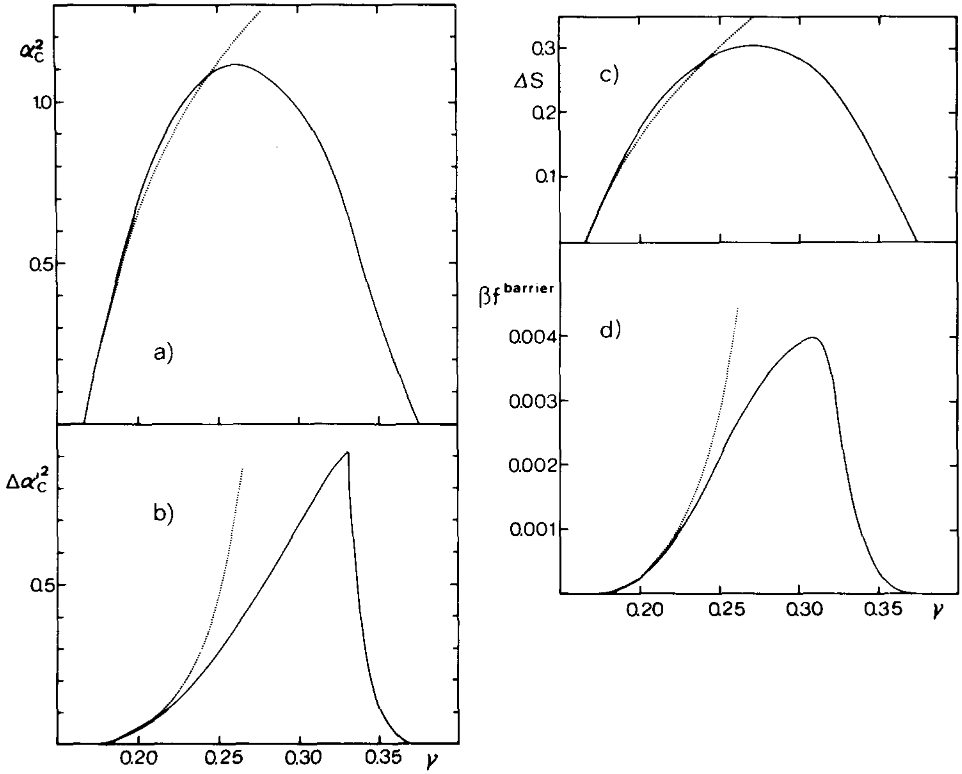

Fig. 3. Properties of the first-order regime at the mean-field level as a function of γ: (a), (b) = jump in order parameters, (c) = entropy jump, (d) = barrier height. The dotted lines show the small α, α' expansions of subsect. 2.2., eqs. (37), (39) (corresponding to the dotted line (1) in fig. 1).

phase diagram is displayed in fig. 1. The fat line running from $(\beta, \gamma) = (\frac{1}{3}, \frac{1}{6})$ to $(0.229, 0.375)$ indicates first-order transitions. The dashed lines are boundaries of the region of metastability. The dotted lines are the analytic approximations discussed in the previous section.

In fig. 3a–d, we show the jumps of the order parameters, the entropy jump and the barrier height at β_c as functions of γ. At $\gamma \approx 0.275$ the entropy jump reaches its maximum, $\Delta s \approx 0.3$. (The dotted lines show again the analytic approximations of subsect. 2.2.).

A few comments may be useful concerning the universality class of the tricritical points. The lower one has two complex fields u, v going from a U(1) symmetric state to a symmetry broken state. It is therefore in the same universality class as the $n = 2$ O(n) symmetric field theory $m^2|\psi|^2 + g|\psi|^4 + \lambda|\psi|^6$ with vanishing g. Near the upper tricritical point in the ordered phase the U(1) symmetry is broken down to Z_2, due to the condensation of the lines of strength-2 ($v \neq 0$). The universality class is therefore the same as for a $n=1$ real field theory, $m^2\varphi^2 + g\varphi^4 + \lambda\varphi^6$, with vanishing g.

3. Monte Carlo simulations

In order to check the validity of our mean field calculations for the mixed action XY model we have performed Monte Carlo simulations on simple cubic lattices with periodic boundary conditions. Equilibrium spin configurations were generated using the standard heat-bath algorithm [15]. In order to save computer time, the group U(1) was approximated by its discrete subgroups Z(16)...Z(32). Since we were looking for a very weak first order transition it was essential to use relatively large lattices from the very beginning. Most information was obtained on 16^3 lattices. The phase diagram in fig. 4 was determined by thermal cycles, varying β or γ in steps of

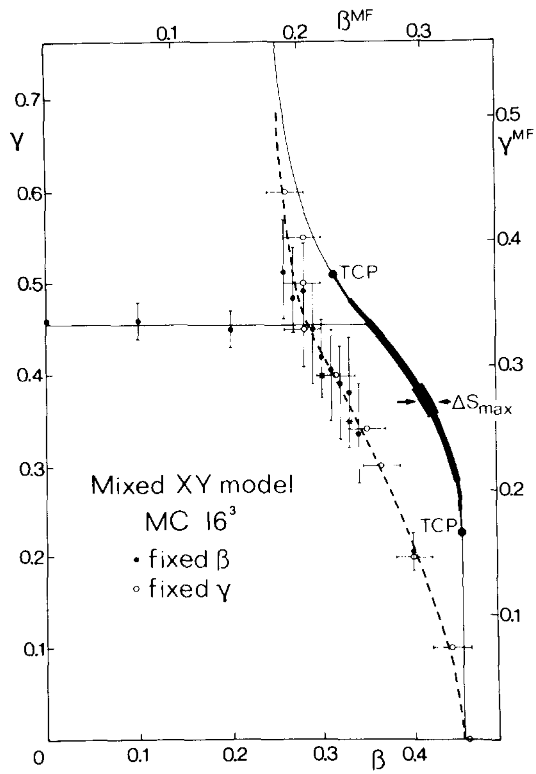

Fig. 4. The phase diagrams as obtained from the Monte Carlo simulations. For comparison we have plotted our mean-field curves, but rescaled in β and γ direction by a factor 0.45/0.33 in order to account heuristically for the fluctuation corrections. The thickness of the mean-field curve is graded according to steps of $\Delta s = 0.1$. The region where Δs is the maximal at the mean-field level was then studied in more detail and found to have a first-order transition also in the fully fluctuating theory.

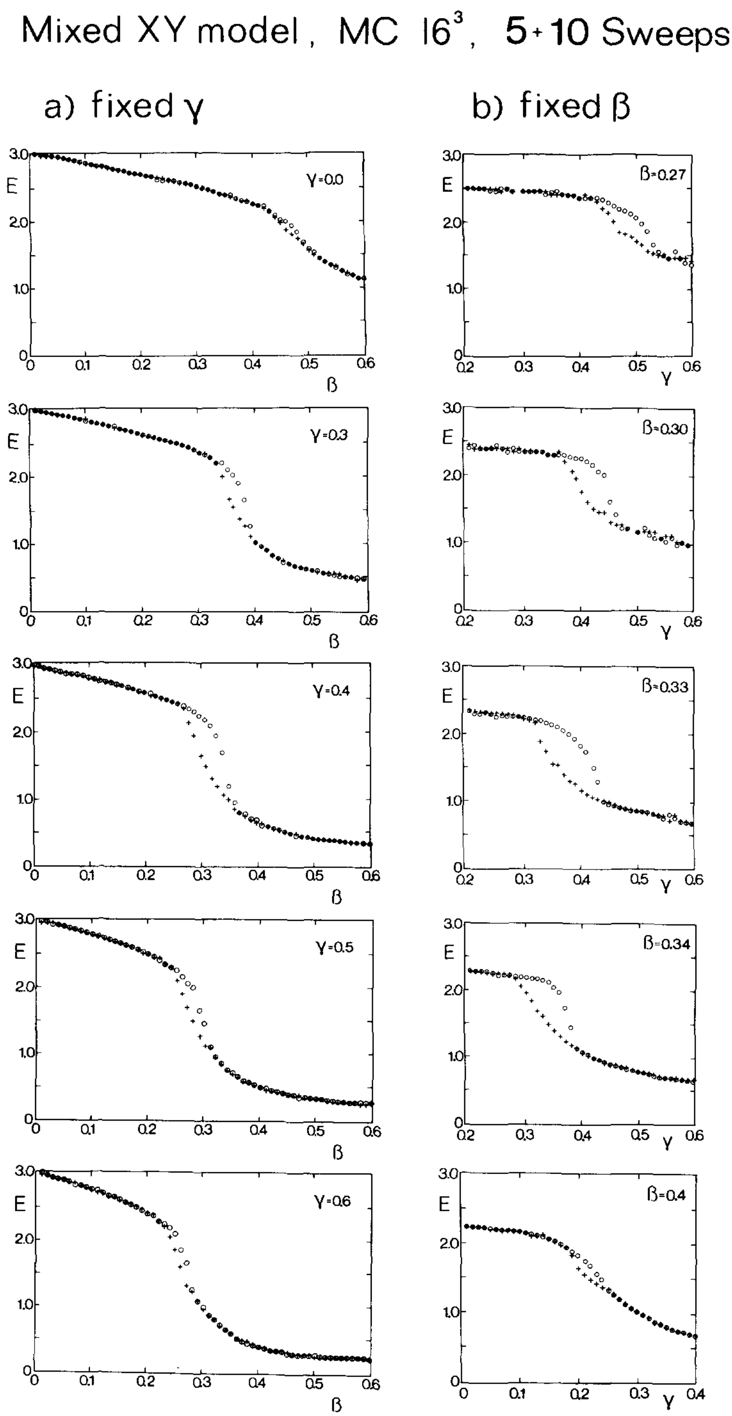

Fig. 5. (a). Thermal cycles in β for various γ showing a pronounced hysteresis at $\gamma \approx 0.30-0.40$, as a rough indication for a first-order transition. (b). Thermal cycles in γ at various fixed β showing a pronounced hysteresis at $\beta \approx 0.30-0.35$.

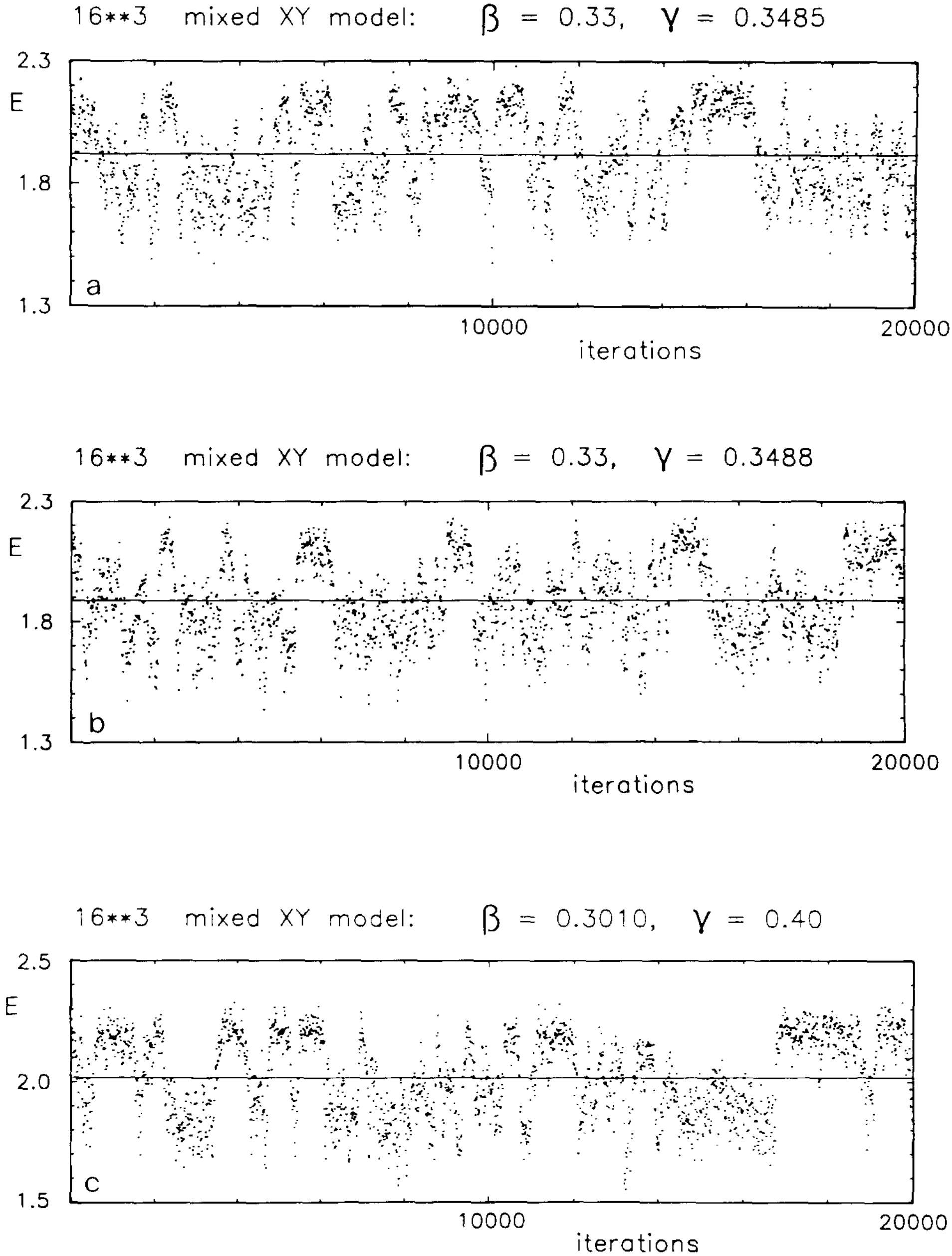

Fig. 6(a)–(c). The time evolution of the internal energy near the phase transition for three slightly different values of β and γ (random starts). They show the jumping back and forth between two minima separated by a barrier typical for a first-order transition. The associated histograms are shown in figs. 7 and 8a.

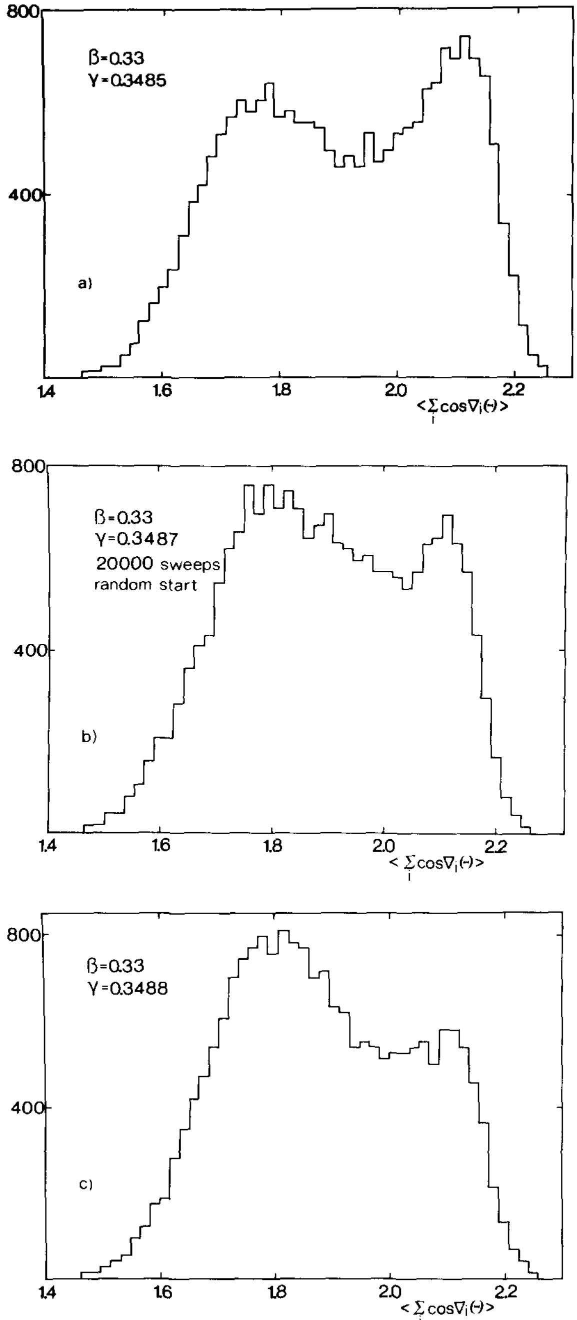

Fig. 7. The histograms of the time evolution of the internal energy $E = \langle \sum_i \cos \nabla_i \theta \rangle$. Fig. 7a and 7c are associated with fig. 6a and 6b, respectively, and fig. 7b is an intermediate situation $\gamma = 0.3487$. There is a clear turnover of a double peak configuration characteristic for a first-order transition.

0.01. At each step we performed 15–50 sweeps through the lattice before going to the next β or γ point using the last 10–35 sweeps for averaging. Since this corresponds to rather rapid heating or cooling we observed in all runs more or less pronounced hysteresis effects. From the center of the hysteresis loops we estimated the critical couplings. In the phase diagram (fig. 4) they are depicted as open (fixed γ) and full (fixed β) circles; the dashed line is only a guide to the eye. The full lines show the corresponding mean-field curves, however, rescaled by a factor 0.45/0.33. After this rescaling, the mean-field curves match the pure XY transition temperatures exactly. The thickness of the first-order mean-field line indicates the size of Δs^{MF}. In fig. 5a, b, some typical thermal cycles are shown which demonstrate that, for both runs with fixed γ or fixed β, the hysteresis effect becomes maximal around

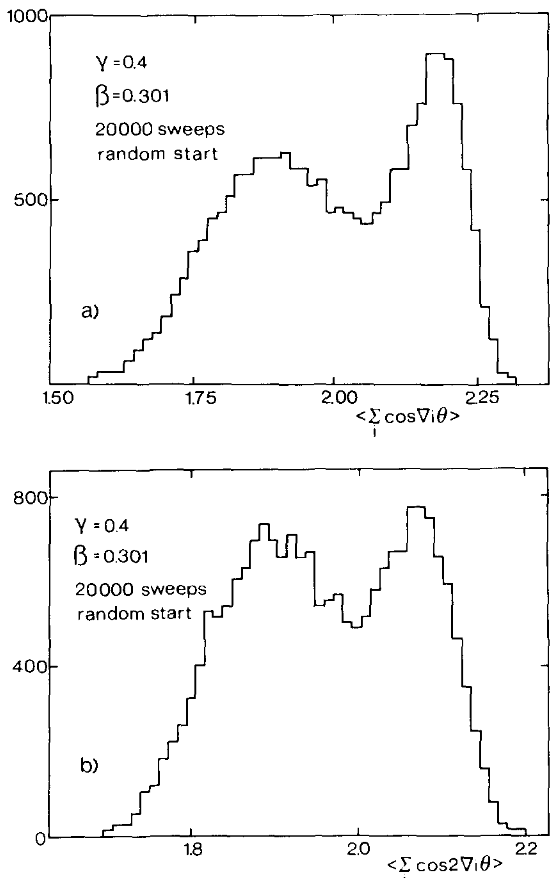

Fig. 8. (a). The histogram of the internal energy of the time evolution, fig. 6c. (b). The histogram for the internal energy with respect to the γ variable $(1/N)\partial(\ln Z)/\partial\gamma = \langle \sum_i \cos(2\nabla_i\theta)\rangle$, at $\gamma = 0.4$, $\beta = 0.301$, which also shows a symmetric double peak characteristic for a first-order transition point.

$\gamma = 0.30, \ldots, 0.40$ and $\beta = 0.30, \ldots, 0.35$, respectively. It is gratifying to note that this range agrees well with the rescaled mean-field prediction (compare fig. 4). Certainly, this observation alone is only a first indication for a first order transition. In order to be sure we have performed at couplings around $\gamma \approx 0.30 - 0.40$, $\beta \approx 0.30 - 0.35$ very long runs (20000 iterations) starting from ordered or random configurations and looked for metastability. Typical results are shown in figs. 6, 7. Fig. 6 gives the time evolution of the average energy which displays transitions between two states. The histograms of these plots are given in figs. 7 and 8d. They show clearly the double peak structures characteristic for a first-order transition. We have checked that these signals do not depend on the initial configuration (total random or ordered lattice) Furthermore, they are confirmed by analogous results for $\langle \Sigma_i \cos(2\nabla_i \theta) \rangle$ (see fig. 8b). From the distance of the two peaks in fig. 7, for $\beta_c = 0.33$ we estimate $\Delta u \approx 0.33$ and $\Delta s = \beta_c \Delta u \approx 0.11$. Comparing with typical entropy jumps of $\Delta s \approx 1 - 2$ in the melting process [3] we see that the transition is only very weakly of first order.

4. Conclusion

We have confirmed that in three dimensions, a mixed action XY model has a first order phase transition. This implies that if one wants to simulate a $|\psi|^4$ theory near its tricritical point, it is not necessary to carry along radial degrees of freedom. The additional piece in the action modifies the effective size fluctuations of the order parameter near the critical point in such a way that it is possible to reach the point of a vanishing quartic coupling. This result should prove to be useful for Monte Carlo studies of Higgs models in four dimensions in which a mixed action of the type (2) for the Higgs system makes it possible to avoid also there the laborious fluctuations of radial degrees of freedom [8].

The authors are grateful to Professors N. Kroll and J. Kuti for their kind hospitality at UCSD.

References

[1] S. Coleman and E.W. Weinberg, Phys. Rev. D7 (1973) 1888;
B.I. Halperin, T.C. Lubensky and S.K. Ma, Phys. Rev. Lett. 32 (1974) 292;
B.I. Halperin and T.C. Lubensky, Sol. State Commun. 14 (1974) 997
[2] A.H. Guth, Phys. Rev. D23 (1981) 347;
A.D. Linde, Rep. Prog. Phys. 47 (1984) 925
[3] H. Kleinert, Lett. Nuovo Cim. 34 (1982) 464
[4] H. Kleinert, Lett. Nuovo Cim. 35 (1982) 405
[5] H. Kleinert, Phys. Lett. 93A (1982) 86
[6] C. Dasgupta and B.I. Halperin, Phys. Rev. Lett. 47 (1981) 1556
[7] J. Bartholomew, Phys. Rev. B28 (1983) 5378;
Y. Munehisa, Phys. Lett. 155B (1985) 159

[8] H. Kühnelt, C.B. Lang and G. Vones, Nucl. Phys. B230 [FS10], (1981) 16;
J. Jersák, C.B. Lang, T. Neuhaus and G. Vones, Aachen preprint PITHA 85/5 (1985) and references therein
[9] J. Jersák, T. Neuhaus and P. Zerwas, Phys. Lett. 133B (1983) 103;
H.G. Everts, J. Jersák, T. Neuhaus and P. Zerwas, Nucl. Phys. B251 [FS13] (1985) 279
[10] W. Janke and H. Kleinert, Nucl. Phys. B 270 [FS16] (1986) 135
[11] J.M. Drouffe and J.-B. Zuber, Phys. Reports 102 (1983) 1
[12] E. Dagotto, Phys. Rev. D30 (1984) 1276
[13] V. Alessandrini and Ph. Boucaud, Nucl. Phys. B225 [FS9] (1983) 303;
E. Brézin, J.C. Le Guillou and J. Zinn-Justin, *in* Phase transitions and critical phenomena, eds. C. Domb and M.S. Green (Academic Press, New York, 1976) vol. 6
[14] H. Kleinert, Gauge theory of stresses and defects (Gordon and Breach, New York, 1986); Phys. Lett. 93A (1982) 86
[15] M. Creutz, L. Jacobs and C. Rebbi, Phys. Reports 95 (1983) 201